EPJ Web of Conferences **3**, 04006 (2010)
DOI:10.1051/epjconf/20100304006

Elastic proton scattering on tritium below the n-^{3}He threshold

R. Lazauskas[1,a]

IPHC, IN2P3-CNRS/Université Louis Pasteur BP 28, F-67037 Strasbourg Cedex 2, France

Abstract. Microscopic calculations using Faddeev-Yakubovski equations in configuration space are performed for low energy elastic proton scattering on ^{3}H nucleus. Realistic nuclear Hamiltonians are used. Coulomb repulsion between the protons as well as isospin breaking effects are rigorously treated.

1 Introduction

Three- and four-nucleon systems provide the testing ground for studying the nuclear interaction. The modern nucleon-nucleon (NN) potentials have reached a very high degree of accuracy in describing the two-nucleon data, thus well constraining the on-shell part of the NN interaction. Nevertheless determination of the off-shell properties and three-nucleon interaction (3NI) in particular, which can be tested only in A≥3 nuclei, remains a highly nontrivial task.

Low energy three-nucleon scattering observables are quite insensitive to 3NI effects. Furthermore three-nucleon dynamics is relatively rigid once deuteron and triton binding energies are fixed. The four nucleon continuum states, containing sensible structures as thresholds and resonances, can show a stronger dependence on the interaction models. The ^{4}He continuum combining total isospin T=0, T=1 and T=2 states, is the richest four-nucleon structure.

In this presentation elastic proton scattering on ^{3}H nucleus is studied between p-^{3}H and n-^{3}He thresholds, in the energy region where α-particles first excited state is imbedded in the continuum. For this aim Faddeev-Yakubovski equations are solved in configuration space, fully considering effects due to the isospin breaking and rigorously treating Coulomb interaction. Different realistic nuclear Hamiltonians are tested, elucidating open problems in nuclear interaction description.

2 Equations

Faddeev-Yakubovski (FY) equations in configuration space [1,2] are used in order to solve four-nucleon problem. In FY formalism four-particle wave function is written as a sum of 18 amplitudes. From those we distinguish amplitudes of type $K^l_{i,j,k}$, which incorporate in their asymptotes 3+1 particle channels, while amplitudes of type H^{kl}_{ij} contain asymptotes of 2+2 particle channels. By interchanging order of the particles one can construct twelve different amplitudes of the type K and six amplitudes of the type H. Introducing isospin quantum number protons and neutrons are treated as the two independent projections of the same particle nucleon with a mass fixed to $\hbar^2/m = 41.47$ MeV·fm^2. Using formalism of isospin twelve amplitudes of type K (as well as six amplitudes of type H) become formally identical and thus only one amplitude of each type K and H are retained. Amplitudes with different order of particle indexing are connected using particle permutation operators P_{ij}, further one employs four combinations of these operators: $P^+ = (P^-)^{-1} \equiv P_{23}P_{12}$, $Q \equiv -P_{34}$ and $\tilde{P} \equiv P_{13}P_{24} = P_{24}P_{13}$. Finally, the original FY [2] equations are slightly modified in order to treat long range Coulomb interaction as well as three nucleon force, which is decomposed into a symmetric sum $V_{123} = V^3_{12}+V^1_{23}+V^2_{31}$. These equations read as:

$$\left(E - H_0 - V_{12} - \sum_{i<j} V^C_{ij}\right) K = V_{12}(P^+ + P^-)\left[(1+Q)K + H\right] + \frac{1}{2}\left(V^1_{23} + V^2_{31}\right)\Psi,$$

$$\left(E - H_0 - V_{12} - \sum_{i<j} V^C_{ij}\right) H = V_{12}\tilde{P}\left[(1+Q)K + H\right],$$

where V_{ij} and V^C_{ij} are, respectively, the short-ranged part and the Coulomb-dominated long-range part of the interaction between the i-th and j-th nucleons. In terms of the FYAs, the total wave function of an $A = 4$ system is given by

$$\Psi = \left[1 + (1 + P^+ + P^-)Q\right](1 + P^+ + P^-)K + (1 + P^+ + P^-)(1 + \tilde{P})H. \quad (1)$$

We expand K and H in terms of the tripolar harmonics $Y^\alpha_i(\hat{x}_i, \hat{y}_i, \hat{z}_i)$, which comprise spins and isospins of the nucleons as well as angular momentum variables,

$$\Phi_i(\mathbf{x}_i, \mathbf{y}_i, \mathbf{z}_i) = \sum_\alpha \frac{\mathcal{F}^\alpha_i(x_i, y_i, z_i)}{x_i y_i z_i} Y^\alpha_i(\hat{x}_i, \hat{y}_i, \hat{z}_i), \quad (2)$$

[a] e-mail: rimantas.lazauskas@ires.in2p3.fr

where Φ stands for either K or H, and the subscript i denotes the particle-grouping class (among the four nucleons).

The partial components $\mathcal{K}_i^{LST}$ and $\mathcal{H}_i^{LST}$ are expanded in the basis of cubic or quintic B-splines. One thus converts integro-differential equations into a system of linear equations. More detailed discussion on the numerical method and equations used can be found in [3].

3 Discussion

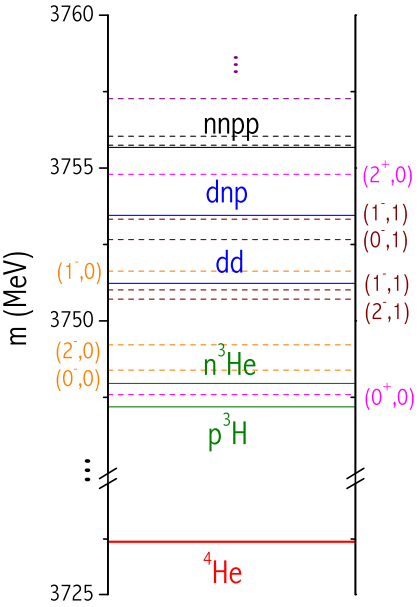

Fig. 1. The experimental spectra of ^{4}He as obtained using R-matrix analysis [4]. In this figure resonances are indicated by the dashed lines.

We consider proton scattering on ^{3}H nuclei for incident (laboratory) proton energies up to E_p =1 MeV, that is below n-^{3}He threshold. This turns to be a very delicate region due to the presence of the first excitation of the α particle (0_2^+), physically situated, just above p-^{3}H threshold, see Fig. 1. Due to difficulty of treating continuum problem this state has been often regarded as a bound one [5]. Nevertheless it turns to be a rather rough approximation, which smears this state over the width of this s-wave Coulomb resonance, covering almost entire region between the n-^{3}He and p-^{3}H thresholds. Indeed, this resonant state slides below the common n-^{3}He and p-^{3}H threshold if Coulomb repulsion between the protons is ignored or if the nucleon-nucleon interaction is taken as an isospin average of n-n, n-p and p-p interactions, without distinguishing n-n and p-p pairs [6].

Subthreshold scattering cross section is very sensitive to the precise position of this (0_2^+) resonance. Actually, the width of the resonance is strongly correlated with its position relative to the p-^{3}H threshold. If this state is slightly overbound the resonance peak in the excitation curve is naturally shifted to the lower energies and becomes more narrow. In case of underbinding one will have much broader resonance, reflected in the flat excitation curve $\frac{d\sigma}{d\Omega}(E,\theta)$ as a function of energy. Very accurate description of the resonant scattering is therefore required. In particular, special care should be taken of charge symmetry breaking terms in order to properly separate the p-^{3}H and n-^{3}He thresholds. Our scattering calculations, which do not restrain the total isospin $\mathcal{T}$, fully accounts for the isospin symmetry breaking and thus are perfectly suited.

Six qualitatively different realistic nuclear Hamiltonians have been tested in this work: local configuration space potential of Argonne group AV18 [7], non-local configuration space potentials INOY (referred as IS-M model in [8] or INOY04' in [9,10]) and ISUJ [12], as well as chiral effective field theory based potential of Idaho group derived up to next-to-next-to-next-to-leading order (I-N^{3}LO) [13]. Urbana three-nucleon interaction was also used in conjunction with AV18 and I-N^{3}LO potentials. The parametrization, commonly called UIX [14], of this three-nucleon interaction was used together with AV18 NN potential; the two-pion exchange parameter has been assigned slightly different value $A_{2\pi}$=-0.03827 MeV when using this force in conjunction with I-N^{3}LO potential. The last adjustment has been made in order to fit the triton binding energy to its experimental value in a model we refer I-N^{3}LO+UIX*.

Performed calculations have been checked for partial wave convergence. In this aim partial wave expansion has been truncated for a certain maximal value of partial angular momenta allowed in the expansion $j_{max} = max(j_x, j_y, j_z)$ for amplitudes K and $j_{max} = max(j_x, j_y, l_z)$ for amplitudes H, where j_x, j_y, j_z and l_z are the partial angular momenta as explained in [11]. In Table 1 convergence for p-^{3}H scattering length calculations with INOY potential are presented. Convergence pattern is not regular, however final results seem to be converged at 0.5% level.

Table 1. Convergence of p-^{3}H scattering length as a function of the maximal value of the partial angular momenta (j_{max}) allowed in the partial wave expansion of FY components. Results are presented for the calculations with INOY potential.

j_{max}	$B(^3\mathrm{H})$	a_0	a_1
1	8.049	1.070	5.051
2	8.402	-30.65	5.583
3	8.481	-37.01	5.452
4	8.482	-36.87	5.377
5	8.483	-37.16	5.371
6	8.483	-37.35	

Results for three-nucleon and α particle binding energies along with p-^{3}H scattering lengths are summarized in Table 2. The binding energy results agree perfectly with the ones obtained using alternative ab-initio methods. The p-

^{3}H scattering lengths presented in the table comprise some small error of 0.02 fm for the singlet scattering length and 0.01 fm for the triplet one. This uncertainty is due to the fact that numerical calculations have been performed for incident proton energies $E_p > 7$ keV and then extrapolated to get corresponding scattering length at $E_p = 0$.

Table 2. Nuclear model predictions for bound state energies in MeV and with p-^{3}H scattering lengths in fm.

Model	B(^{3}H)	B(^{3}He)	B(^{4}He)	$a_0(p^3\mathrm{H})$	$a_1(p^3\mathrm{H})$
ISUJ	8.482	7.718	28.91	-35.5	5.39
INOY	8.483	7.720	29.08	-37.4	5.37
AV18	7.623	6.925	24.23	-15.5	5.79
AV18+UIX	8.483	7.753	28.47	-23.6	5.47
I-N^{3}LO	7.852	7.159	25.36	-19.6	5.85
I-N^{3}O+UIX*	8.482	7.737	28.12	-22.9	5.59
Exp.	8.482	7.718	28.30		

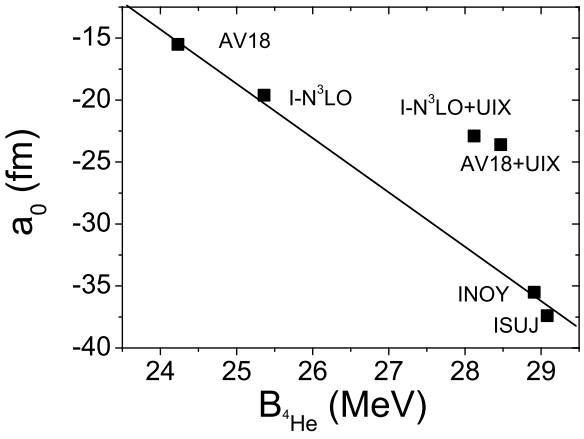

Fig. 2. Variation of the p-^{3}H singlet scattering length with the binding energy of α particle. Linear correlation is observed for the models non-containing three-nucleon force.

In figure 2 the obtained singlet p-^{3}H scattering length is presented as a function of α particle binding energy. One can see linear correlation for model results without three-nucleon force: singlet scattering length decreases when increasing binding of the α particle. It indicates that (0_2^+) excitations moves together with the ground state with respect to p-^{3}H threshold. The linear correlation is broken once three nucleon force is added, one should note that the similar effect is affirmed by Nogga et al. [15] for the correlation between the binding energies of α particle and triton (^{3}H).

The p-^{3}H triplet channel ($J^\pi = 1^+$) is repulsive, while variation of the p-^{3}H triplet scattering length is rather moderate: this scattering length tends to decrease as the three-nucleon binding energy increases. Correlation is not perfect, in particulary results for momentum space I-N^{3}LO potential tends to break the correlation. Probably it is due to the fact that for this potential we have used point-Coulomb repulsion, while the configuration space potentials employ screened Coulomb interaction having the same parametrization as the one encoded in EM part of the AV18 proton-proton potential.

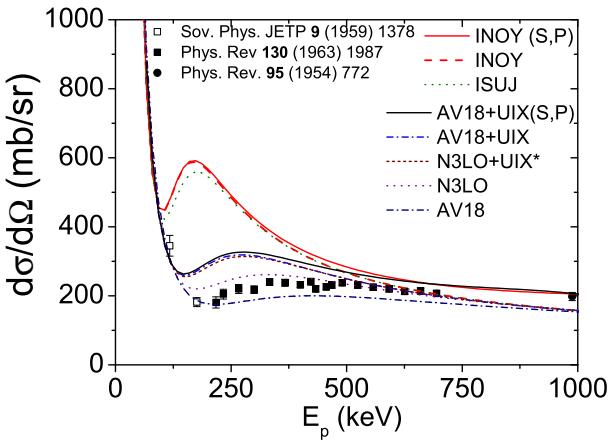

Fig. 3. Various model calculations for p-^{3}H excitation function $\frac{d\sigma}{d\Omega}(E)\big|_{\theta_{c.m.}=120^\circ}$ compared with experimental data from [19,17, 18].

Figure 3 compares calculated p-^{3}H differential cross section at $\theta_{c.m.}$=120° with experimental data from [19,17, 18]. For proton energies, below 100 keV, scattering cross section diverges due to the effective Coulomb repulsion between the proton and triton. This analytical behavior hides completely strong interaction effects. Only beyond 100-150 keV nuclear scattering amplitudes are pronounced, revealing the clear resonant behavior of the singlet channel ($J^\pi = 0^+$), even though this wave is suppressed by the statistical factor 3 compared to the triplet ($J^\pi = 1^+$) one. The resonant peak is strongly enhanced by INOY and ISUJ models, which overbinding α particle ground state also places its (0_2^+) excitation too close to the p-^{3}H threshold. The resonance width naturally increases as resonance moves further into continuum – therefore other model predicted excitation functions ($\frac{d\sigma}{d\Omega}(E, \theta_{c.m.} = 120°)$) are much flatter than INOY or ISUJ ones. The best, however not perfect, description of the experimental data in the resonance region (E_p ~200-600 keV) is achieved by I-N3LO model. The AV18 Hamiltonian slightly underestimates experimental cross section below 600 keV, while its excitation function is too flat. Inclusion of Urbana type three nucleon force makes I-N3LO+UIX* and AV18+UIX model results almost indiscernible, while the elastic cross section is visibly overestimated in the resonance region. The agreement between two model predictions is probably coincidental, as Hale and Hofmann[21] demonstrated strong sensitivity of the p-^{3}H cross section to the 3NF parameters. Qualitatively the same behavior is observed, when analyz-

ing the differential cross section as a function of the scattering angle. It is demonstrated in the figure 4 for the incident protons of 300 keV.

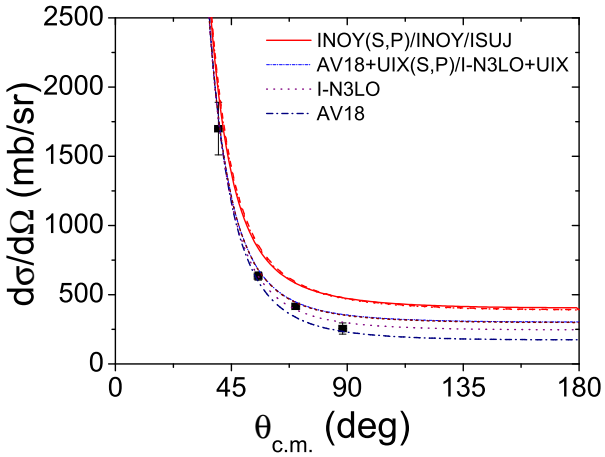

Fig. 4. Calculated p-^{3}H differential cross sections are compared with experimental data of [20] for incident proton energies of 0.3 MeV.

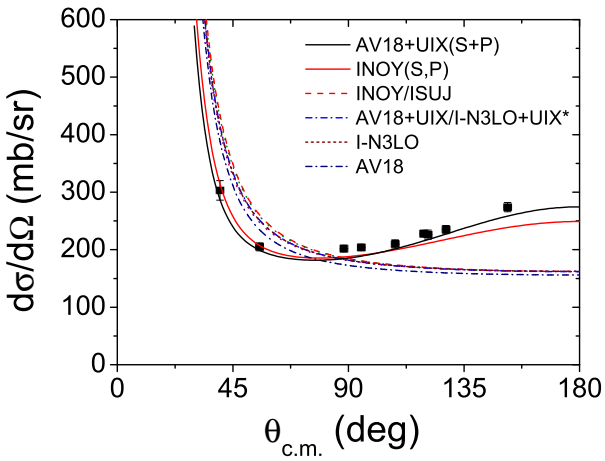

Fig. 5. Calculated p-^{3}H differential cross sections are compared with experimental data of [20] for incident proton energies of 0.9 MeV.

Beyond the resonance region the S-wave cross section predicted by all models coincide into monotonic decreasing curve. The AV18 model gives broadest (0^+_2) resonance, therefore it integrates the joint curve the last, only for incident proton energies around 1 MeV. Several P-wave resonances are also present in ^{4}He continuum with centers situated just above n-^{3}He threshold, see Fig. 1. These resonances, and in particular a narrow $J^\pi = 0^-$ one, has tails emerging already from the region below n-^{3}He threshold. Negative parity states therefore are imperative for the description of the scattering cross section already beyond $E_p \approx 400$ keV, making calculations largely involved. Calculations including P-waves have been performed only for INOY and AV18+UIX models. P-waves seems to improve agreement with experimental data measured close to n-^{3}He threshold and in particular angular distributions of the backward scattered protons. See the figure 5 for incident protons of 900 keV, which is only ~100 keV below n-^{3}He threshold. Backward scattering cross section is slightly underestimated by INOY potential, indicating that negative parity resonances are displaced to the higher energies by this interaction. Similar observation has been made by Deltuva et al. [16] for low energy n-^{3}He scattering. It is obvious that NN P-waves should have a strong impact for the negative parity states of the nuclear system and therefore stronger NN P-waves than those given by the INOY model are preferred by the experimental data. On the other hand AV18+UIX model describes almost perfectly differential cross section at 900 keV, which is mostly due to much larger $J^\pi = 0^-$ phaseshift than one obtained using INOY. Interplay of different P-waves can be best studied using analyzing power data, unfortunately no such data exist for p-^{3}H system below E_p=4 MeV.

Interplay of negative and positive parity resonances in ^{4}He continuum presents an ideal laboratory to fine tune the two and three nucleon interactions. In particular, the p-^{3}H scattering at very low energies, permits to test the charge symmetry breaking in NN S-waves. At higher energies close to n-^{3}He threshold contribution of negative parity states to the scattering process can be well separated from the contribution of the positive parity ones. Negative parity states turns to demonstrate stronger sensitivity to NN P-waves. Furthermore if the study of the ^{4}He continuum is undertaken in parallel with resonant scattering in n-^{3}H and p-^{3}He systems the new frontiers opens to understand isospin symmetry of NN P-waves as well as isospin structure of the three-nucleon interaction. Success of this campaign relies strongly on the abundance and quality of the low energy experiments for four nucleon system. In particular the nucleon scattering data on tritium is very scarce, while the tritium experiments have been completely abandoned for the last 30 years.

4 Conclusion

Recent results on p-^{3}H elastic scattering are presented for the incident proton energies up to 1 MeV. Calculations have been performed solving Faddeev-Yakubovski equations in configuration space, which incorporate Coulomb and fully accounts for isospin breaking effects in nuclear interaction. Converged results are presented for six realistic nuclear Hamiltonians. None of the tested Hamiltonians, even ones supplemented with UIX-type three-nucleon force, have been able to reproduce the shape of the nearthreshold $J^\pi = 0^+$ resonance together with the ground state binding energy of the α particle.

The accurate theoretical calculations for low energy four-nucleon scattering are now performed by several groups and proves themselves to be strongly reliable. Therefore ^{4}He continuum turns to be an ideal laboratory to test and fine tune the two and three nucleon interaction models: in particular, this system is crucial in understanding the charge symmetry breaking. In this perspective new four-nucleon scattering experiments at low energies are strongly anticipated.

Acknowledgement

This work was granted access to the HPC resources of IDRIS under the allocation 2009-i2009056006 made by GENCI (Grand Equipement National de Calcul Intensif). We thank the staff members of the IDRIS for their constant help.

5 Bibliography

References

1. L.D. Faddeev: Zh. Eksp. Teor. Fiz. **39**, (1960) (Wiley & Sons Inc., 1972). 1459 [Sov. Phys. JETP **12**, (1961) 1014].
2. O. A. Yakubowsky, Sov. J. Nucl. Phys. **5** (1967) 937.
3. R. Lazauskas, PhD Thesis Université Joseph Fourier, Grenoble (2003); http://tel.ccsd.cnrs.fr/documents/archives0/00/00/41/78/
4. D.R. Tilley, H.R. Weller and G.M. Hale, Nucl. Phys. A**541** (1992) 1.
5. E. Hiyama, B. F. Gibson and M. Kamimura, Phys. Rev. C **70** (2004) 031001.
6. A. C. Fonseca, G. Hale and J. Haidenbauer, Few-Body Syst **31** (2002) 139.
7. R.B. Wiringa, V.G.J. Stoks, R. Schiavilla, Phys. Rev. **C51** (1995) 38.
8. P. Doleschall, Phys. Rev. **C69** (2004) 054001.
9. A. Deltuva and A. C. Fonseca, Phys. Rev. C **75**, 014005 (2007) [arXiv:nucl-th/0611029].
10. R. Lazauskas and J. Carbonell, Phys. Rev. C **70** (2004) 044002 [arXiv:nucl-th/0408048].
11. R. Lazauskas, J. Carbonell, A. C. Fonseca, M. Viviani, A. Kievsky and S. Rosati, Phys. Rev. C **71**, 034004 (2005) [arXiv:nucl-th/0412089].
12. P. Doleschall, Phys. Rev. **C77** (2008) 034002.
13. D. R. Entem and R. Machleidt, Phys. Rev. **C68** (2003) 041001(R).
14. B.S. Pudliner, V.R. Pandharipande, J. Carlson and R.B. Wiringa, Phys. Rev. Lett. **74** (1995) 4396.
15. A. Nogga, H. Kamada, W. Gloeckle and B. R. Barrett, Phys. Rev. C **65** (2002) 054003 [arXiv:nucl-th/0112026].
16. A. Deltuva and A. C. Fonseca, Phys. Rev. C **76** (2007) 021001(R) [arXiv:nucl-th/0703066].
17. E. M. Ennis and A. Hemmendinger, Phys. Rev. **95** (1954) 772.
18. Y. G. Balashko et al., Sov. Phys. JETP **9** (1959) 1378.
19. N. Jarmie et al., Phys. Rev. **130** (1963) 1987.
20. Y. G. Balashko et al., Journ. Izv. Rossiiskoi Akademii Nauk, Ser. Fiz. **28** (1964) 1124; Proc. Nuclear Physics Congress, Paris (1964) 255.
21. H. M. Hofmann and G. M. Hale, Phys. Rev. C **77**, 044002 (2008) [arXiv:nucl-th/0512065].